RSC Advances

PAPER

View Article Online
View Journal | View Issue

Cite this: *RSC Adv.*, 2014, **4**, 36896

An analytical model and ANN simulation for carbon nanotube based ammonium gas sensors

Elnaz Akbari,[a] Zolkafle Buntat,*[a] Aria Enzevaee,[b] Seyed Javad Mirazimiabarghouei,[c] Mahdi Bahadoran,[d] Ali Shahidi[e] and Ali Nikoukar[f]

Received 26th June 2014
Accepted 4th August 2014

DOI: 10.1039/c4ra06291d

www.rsc.org/advances

As one of the most interesting advancements in the field of nano technology, carbon nanotubes (CNTs) have been given special attention because of their remarkable mechanical and electrical properties and are being used in many scientific and engineering research projects. One such application facilitated by the fact that CNTs experience changes in electrical conductivity when exposed to different gases is the use of these materials as part of gas detection sensors. These are typically constructed on a Field Effect Transistor (FET) based structure in which the CNT is employed as the channel between the source and the drain. In this study, an analytical model has been proposed and developed with the initial assumption that the gate voltage is directly proportional to the gas concentration as well as its temperature. Using the corresponding formulae for CNT conductance, the proposed mathematical model is derived. An Artificial Neural Network (ANN) algorithm has also been incorporated to obtain another model for the *I*–*V* characteristics in which the experimental data extracted from a recent work by N. Peng *et al.* has been used as the training data set. The comparative study of the results from ANN as well as the analytical models with the experimental data in hand show a satisfactory agreement which validates the proposed models. It is observed that the results obtained from the ANN model are closer to the experimental data than those from the analytical model.

1. Introduction

With the development of industry and human activity, air pollution has become a serious problem for the environment. Hazardous gases such as NO_2, NH_3, CO, H_2S, and SO_2 have harmful effects on human life, animals, and plants. Therefore, it is essential to develop gas sensors with high sensitivity in order to detect harmful gases for the purpose of improving the quality of environmental living conditions and protecting humans from exposure to hazardous gases.[1,24]

Sensor is a term used for devices that can measure specific physical quantities and convert them into a readable electrical signal for an observer or an instrument. Sensors come in many different types based on the intended material that they are expected to detect as well as mechanisms of detection. They can be classified as electromagnetic sensors, mechanical sensors, thermal sensors, *etc.*[7,15] The trend in sensor manufacturing and production is heading toward those with higher sensitivities, better selectivities and faster response times; also those which are easier to fabricate, more portable, remotely operateable and more cost-effective are more desirable.[34] In addition to the main sensing function, the sensor is expected to keep track of various ambient factors such as temperature and humidity, time, location and event history. Rapid improvements in nanoscience and engineering, as well as faster and more advanced compact integrated electronics are helping these requirements come true. In this regard, many newly developed materials like graphene and carbon nanotubes (CNTs) are now becoming available for the design fabrication of nanosensors.[18]

To date, carbon nanotubes based gas sensors have aroused great interest since their discovery in 1991. Carbon nanotubes are formed in two major types; single-walled carbon nanotubes (SWNTs) comprising single graphene sheet wrapped in the form of a cylindrical tube and multi-walled carbon nanotubes (MWNTs) consisting of a group of such nanotubes in concentric configuration, both possessing varying inherent band gaps (Fig. 1).[21,41]

Depending on their helicity, carbon nanotubes are either electrically conductive or semi-conductive. They possess unique intrinsic properties including high surface area, high chemical and mechanical stability and excellent electrical conductivity.

[a]*Institute of High Voltage & High Current, Faculty of Electrical Engineering, Universiti Teknologi Malaysia, Johor Bahru, 81310 Malaysia. E-mail: zolkafle@fke.utm.my*
[b]*Faculty of Mechanical Engineering, Universiti Teknologi Malaysia, Johor Bahru, 81310 Malaysia*
[c]*School of Mechanical and Electrical Engineering, USQ Faculty of Health, Engineering and Sciences, Toowoomba, Queensland, Australia*
[d]*Institute of Advanced Photonics Science, Nanotechnology Research Alliance, Universiti Teknologi Malaysia, Johor Bahru 81310, Malaysia*
[e]*RWTH Aachen, Department of Computer Science 4, Ahornstr. 55, 52056 Aachen, Germany*
[f]*Faculty of Computing, Universiti Teknologi Malaysia, Johor Bahru 81310, Malaysia*

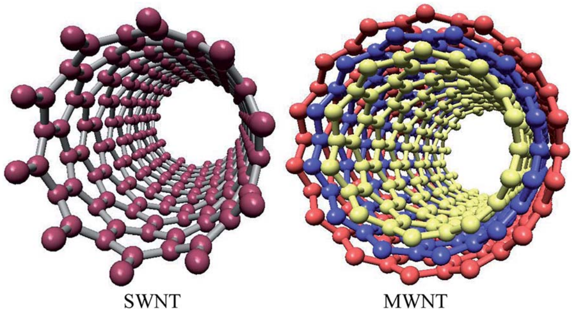

Fig. 1 Schematic of different CNT structures.

Moreover, SWNTs with diameters as low as ~1 nm and near-ballistic electron transport,[9,16,39] makes them an ideal candidate for sensing/transducer material for direct electronic detection of analyte gases. This plethora of unique properties of SWNTs has motivated researchers across the globe to pursue development of SWNTs based gas sensors. The achievements in the application for carbon nanotubes as arrays or sensors have been well documented and thoroughly reviewed.[10,30,33,38]

Almost a decade ago, Kong *et al.*,[25] and during the same time, Collins *et al.*[11] first demonstrated that the conductance of individual SWNTs can be changed up to three times within a few seconds after they are exposed to electron donating NH_3 and electron withdrawing NO_2 gas at room temperature, with superior sensing performance over commercially available sensors. The mechanism of sensing was based on direct charge transfer between adsorbate and p-type semi conductive SWNTs causing modulation of Fermi level in the semiconducting tubes (Fig. 2).[31]

It is known that the carbon nanotube characteristics depend strongly upon their physical features such as chirality and diameter.[46] Single-walled nanotubes are typically categorized as either metallic or semiconductors according to their chirality. Semiconducting SWNTs can be used in the fabrication of FET devices able to be operated at room temperature and under ambient conditions.[13,42]

It has been demonstrated that semiconducting SWNTs experience significant changes in conductance levels in the presence of different gases. As depicted in Fig. 3, the proposed gas sensor using CNT as the conducting channel has a structure quite similar to that of the conventional metal-oxide semiconductor field effect transistor (MOSFET) which consists of one source metal, one drain metal, a silicon back gate as well as a gate insulator.[20,22] The source and drain electrodes are connected by a CNT channel, while a dielectric barrier layer separates the channel from the gate. In most studies in the literature, silicon is used as the back gate, while SiO_2 serves as a dielectric layer.[26,36] When gas molecules are in contact with the CNT surface, carrier concentration will undergo a change owing to the variability of the current between the drain and the source which is a measurable parameter.[32]

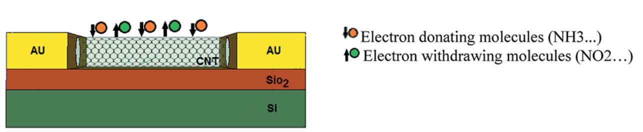

Fig. 2 Schematic of molecules donating and withdrawing electrons on CNT.

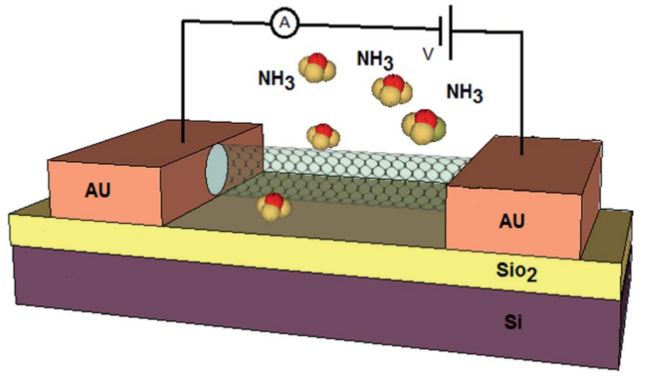

Fig. 3 FET based gas sensor structure.

In order to carry out a comparative study, it has been attempted to implement an artificial intelligence method to develop another model. Artificial Neural Network (ANN) as one of the most accurate and powerful intelligent schemes has been chosen as the tool in this step. The results obtained from the constructed ANN are then compared to those from the analytical model as well as the experimental data to check which approach provides better levels of accuracy.[35,48]

Artificial Neural Networks is an intelligent algorithm which has been developed based on an analogy to biological nervous system. Various types and structures of artificial neural networks have been employed in scientific analytical studies among which, the most common and comprehensible is one consisting of interconnected group of neurons which are mathematical operator units called Perceptrons.[2,27]

A schematic of the typical structure of an ANN comprising Perceptrons is provided in Fig. 4. Each input value to a Perceptron is multiplied by a weight and added to a bias value. The

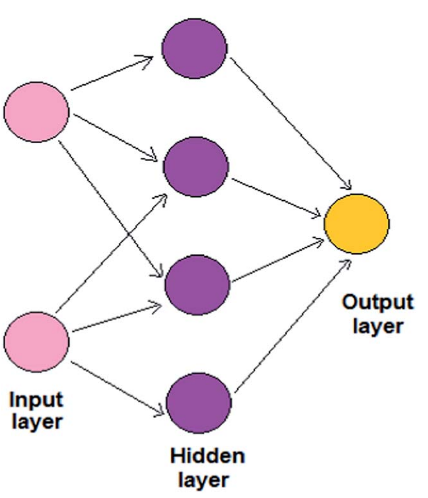

Fig. 4 Simple artificial neural network.

general mechanism of ANN includes a process in which a set of input data are introduced to the network. Through a series of mathematical calculations based on predefined "activation functions" for each neuron or "node", an output value is given by the ANN. In order for the ANN to learn to compute the optimum output value, a training data set is introduced to the network before the actual inputs are given to the artificial neural network.[37,47]

Based on a predefined learning algorithm, the ANN updates the weights and bias corresponding to each node using the error between the calculated results from the actual inputs and the desired output.[17,43] In our study, feed-forward structure for the neural network with Back Propagation learning algorithm has been implemented. The experimental data has been used as the training data set has been employed for validation and testing. The results show satisfactory agreement between the results from the proposed model with the experimental counterparts.

2. Proposed models

2.1 Analytical model

It has been attempted to model the CNT band structure beginning with modeling the single layer graphene band structure. Employing the Taylor series expansion near the Fermi points, the energy dispersion relation can be derived as follows.[3,6]

$$E(k) = \pm\frac{t\ 3a_{\mathrm{c-c}}}{2}\sqrt{\left(\frac{2}{3d}\right)^2 + {k_x}^2} \tag{1}$$

where $a_{\mathrm{c-c}} = 1.42$ Å represents the length of carbon–carbon (C–C) bond, d is the CNT diameter, $t = 2.7$ (eV) denotes the nearest neighbour C–C tight binding overlap energy, and the $\pm$ symbol has been included to account for conductance and valence bands. We can simply write for the first band gap energy $E_g = 2a_{\mathrm{c-c}}t/d = (0.8\ \mathrm{eV})/d$. Also, since the band structure is parabolic near the $k = 0$ points, it can be written:

$$E(k) \approx \frac{E_g}{2} + \frac{\hbar^2 {k_x}^2}{2m^*} \tag{2}$$

where $\hbar$ is the reduced Plank constant, m^* is the effective mass of the CNT depending upon the tube diameter, k_x represents longitudinal wave vector component.[5,8] The number of conduction channels in the energy E is defined as:

$$M(E) = 2\frac{\Delta E}{\Delta k L} = \frac{3\ a_{\mathrm{c-c}}t}{L}\left(\frac{4E}{3\ a_{\mathrm{c-c}}t} - \frac{8}{9d}\right)^{1/2} \tag{3}$$

where L denotes the channel length. Two major factors contribute to the conductance effect on large channels, enabling it to follow the Ohmic scaling law based on Landauer formula. The first factor independent of length is the interface resistance. The second one results from the fact that the relation between the conductance and the width is nonlinear and is dependent upon the number of modes in the conductor. However, these modes are the quantized parameters in the Landauer formula in which both factors are interrelated as demonstrated by eqn (4):[4]

$$G = \frac{2q^2}{h}\int_{-\infty}^{+\infty} \mathrm{d}E M(E)T(E)\left(-\frac{\mathrm{d}f}{\mathrm{d}E}\right) \tag{4}$$

Where h represents the Plank constant, q denotes the electron charge and T is the transmission probability of an injected electron through the channel approximated as $(T(E) = 1)$ in ballistic channels.[12] Owing to the fact that the expression $\frac{\mathrm{d}f}{\mathrm{d}E}$ is noticeable only near the Fermi energy,[12] the conductance can be obtained by considering the Fermi–Dirac distribution function as.[29]

$$G = \frac{2q^2}{h}\frac{3a_{\mathrm{c-c}}t}{L}\left(\frac{4}{3a_{\mathrm{c-c}}t}\right)^{1/2}\int_{-\infty}^{+\infty}\left(E - \frac{2a_{\mathrm{c-c}}t}{3d^2}\right)^{\frac{1}{2}} d\left(-\frac{1}{1+\mathrm{e}^{(E-E_F)/k_BT}}\right) \tag{5}$$

Changing the integral boundaries as follows, eqn (5) can be rewritten as

$$G = \frac{4q^2}{hL}(3a_{\mathrm{c-c}}t\pi k_BT)^{\frac{1}{2}}\left[\int_{-\infty}^{+\infty}\frac{x^{-1/2}}{1+\mathrm{e}^{x-\eta}}\mathrm{d}x + \int_0^{+\infty}\frac{x^{-1/2}}{1+\mathrm{e}^{x+\eta}}\mathrm{d}x\right] \tag{6}$$

Where $x = (E - E_g)/k_BT$ and the normalized Fermi energy is given by $\eta = (E_F - E_g)/k_BT$. This equation can be numerically solved by incorporating the partial integration method.[14,23,45] The general model for the conductance of carbon nanotube-based gas sensor can be derived similar to that of silicon based model proposed by Gunlycke.[19]

$$G = \frac{4q^2}{hL}(3a_{\mathrm{c-c}}t\pi k_BT)^{\frac{1}{2}}\left[\mathscr{I}_{-\frac{1}{2}}(\eta) + \mathscr{I}_{-\frac{1}{2}}(-\eta)\right] \tag{7}$$

The conductance characteristic demonstrates the performance of NH_3 gas sensor based on CNT nanostructure. It has been revealed that when the CNT gas sensor is exposed to NH_3, the conductance changes.[44] We have proposed a model based on the reported experimental data and the relationship between conductance, gas concentration and temperatures follows:[40]

$$G_{\mathrm{wg}} = G_{\mathrm{wog}} + G_{\mathrm{wg}T} + G_{\mathrm{wg}F} \tag{8}$$

When the sensor is exposed to the gases in different temperatures, we can define three parameters for conductance, namely G_{wog}, $G_{\mathrm{wg}T}$ and $G_{\mathrm{wg}F}$. The first parameter, G_{wog}, is the conductance without gas; $G_{\mathrm{wg}T}$ is assumed as the conductivity changes depending on T parameter, and the last parameter, $G_{\mathrm{wg}F}$, is based on different values of gas concentration with constant temperature. It is shown that when CNT gas sensor is exposed to NH_3, the conductance levels changes with respect to temperature and varying concentrations.[35] As E_g results in varying conductance of channel, the parameters that have a strong influence on gas sensor conductance are the gas concentration as well as gas temperature. It has been shown that E_g depends on temperature and gas concentration; therefore, we can write:

$$\begin{Bmatrix} E_g \propto F \\ E_g \propto T \end{Bmatrix} \Rightarrow E_g = \alpha T + \beta F \tag{9}$$

Finally, eqn (9) and (10) are employed to obtain the conductance model of gas sensor as:

$$G_{wog} = \frac{4q^2}{hL}(3a_{c-c}t\pi k_B T)^{\frac{1}{2}}\Big[\mathscr{I}_{\frac{-1}{2}}(((E_g - E_T) \times q)/k_B T) + \mathscr{I}_{\frac{-1}{2}}((-(E_g - E_T) \times q)/k_B T)\Big] \tag{10}$$

$$G_{wg} = \frac{4q^2}{hL}(3a_{c-c}t\pi k_B T)^{\frac{1}{2}}\Big[\mathscr{I}_{\frac{-1}{2}}((\alpha T + \beta F - E_T) \times q/k_B T) + \mathscr{I}_{\frac{-1}{2}}(-(\alpha T + \beta F - E_T) \times q/k_B T)\Big] \tag{11}$$

Based on the current–voltage characteristic of graphene based FET devices, the performance of the gas sensor can be evaluated by eqn (12). Assuming that the source and substrate terminals are kept in ground potential, and applying a small voltage between source and drain (VDS), the channel region experiences a flow of electrons. Moreover, the relationship between current and conductance can be replaced by Fermi–Dirac integral shape of general conductance model of SWCNT as:

$$I = \left[\frac{4q^2}{hL}(3a_{c-c}t\pi k_B T)^{\frac{1}{2}}\Big[\mathscr{I}_{\frac{-1}{2}}((\alpha T + \beta F - E_T) \times q/k_B T) + \mathscr{I}_{\frac{-1}{2}}(-(\alpha T + \beta F - E_T) \times q/k_B T)\Big]\right] \times (V_{gs} - V_t) \tag{12}$$

Where V_{gs} is the voltage between the gate and the source and V_t denotes the threshold voltage. *I–V* characteristic of the proposed model in comparison with experimental results is depicted in figures (a_1) to (g_1). An increase in the current can be associated to the charge transfer between CNT and NH_3 molecules when the NH_3 molecules are the donors. This phenomenon is also known as chemical doping by gas molecules. It clearly gives an illustration of the fact that there is a good agreement between the proposed model and the extracted data.[28] In the suggested model, different temperature and concentration values are demonstrated in the form of α and β parameters, respectively, to create an agreement with reported data which is tabulated as follows (Table 1):

Table 1 Different temperature and concentration values with α and β parameters

T (°C)	F (ppm)	α	β
25	500	−4	0.03
50	500	−2	0.03
100	500	−1	0.03
150	500	−0.8	0.03
200	100	−0.5	0.01
200	200	−0.5	0.02
200	500	−0.5	0.03

According to the analytical model, α is suggested as the temperature control parameter and is obtained by iteration method. The analytical model based on the extracted data in our study shows that the rate of changes in conductivity depending on temperature gives better results by:

$$\alpha = a\ln(T) - b \tag{13}$$

Parameters a and b are extracted as $a = 0.012$ and $b = 0.046$. Also, β defined as a controlled parameter of gas concentration which calculated by iterative method and shows the rate of change in conductivity depends on gas concentration given by:

$$\beta = c\ln(F) - d \tag{14}$$

Where the constants are calculated in the same manner as $c = 1.622$ and $d = 8.814$.

2.2 ANN based model

The proposed Artificial Neural Network has been developed incorporating a network comprising three layers: one input, one output and one hidden layer. The hidden layer consisted of three nodes and feed-forward structure has been employed for the ANN. MATLAB software was utilized for programming and the experimental data were used as the training data set as well

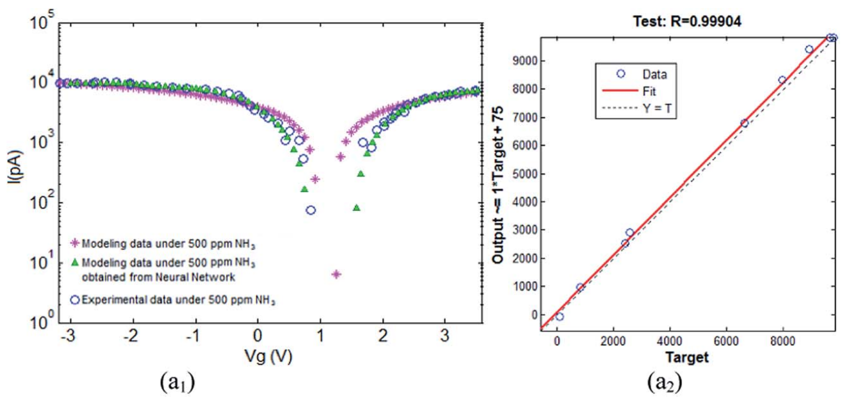

Fig. 5 Comparative study of proposed analytical and ANN models with experimental data under 500 ppm, at 25 °C and corresponding ANN regression graphs (a_2).

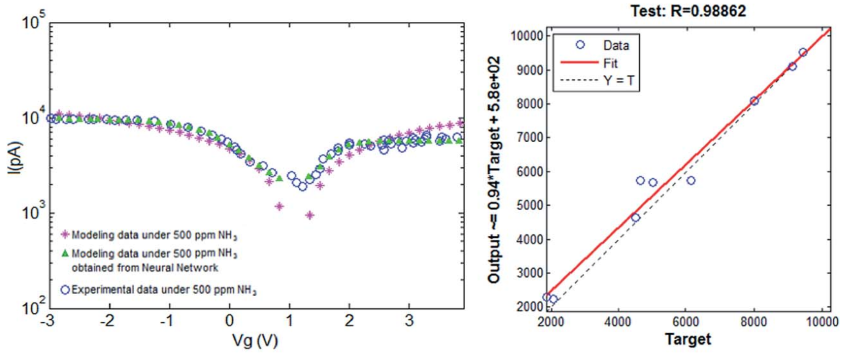

(a₁) (a₂)

Fig. 6 Comparative study of proposed analytical and ANN models with experimental data under 500 ppm, at 50 °C and corresponding ANN regression graphs (a_2).

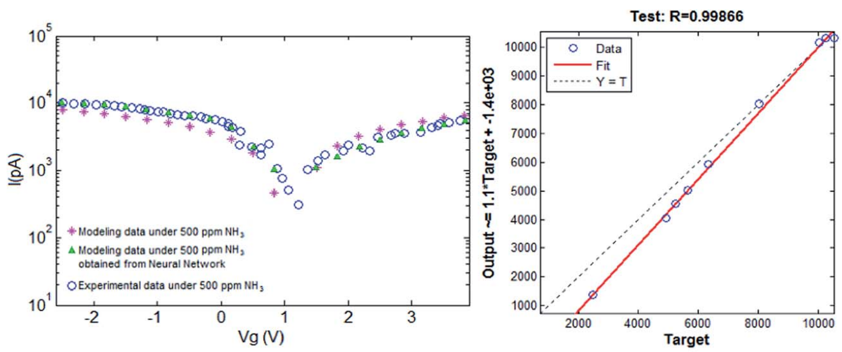

(a_1) (a_2)

Fig. 7 Comparative study of proposed analytical and ANN models with experimental data under 500 ppm, at 100 °C and corresponding ANN regression graphs (a_2).

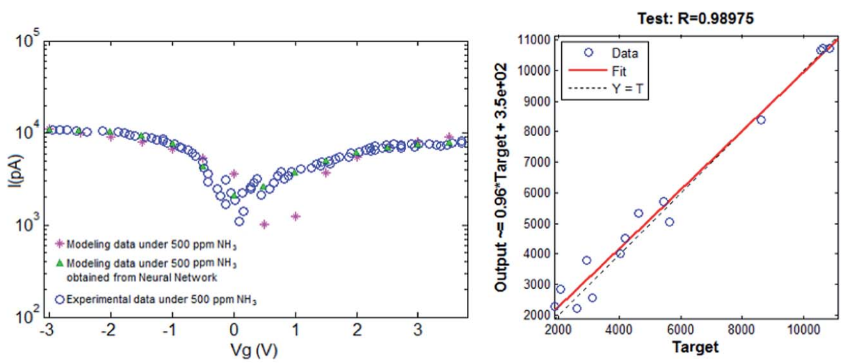

(a_1) (a_2)

Fig. 8 Comparative study of proposed analytical and ANN models with experimental data under 500 ppm, at 150 °C and corresponding ANN regression graphs (a_2).

as testing data. The built-in Neural Network tool in MATLAB randomly selects part of the input data for training and the rest is employed for testing. The values for the weights and bias are also randomly chosen by the software and updated in each epoch using the Back-propagation learning algorithm. For each set of input data, the corresponding plots of the *I*–*V* points as well as the regression graph were plotted. The results are provided in Fig. (5)–(11).

3. Discussion and results

The diagrams depicting the *I*–*V* characteristic of CNT corresponding to different gas temperatures at 500 ppm concentration are illustrated in Fig. (5)–(8). The values associated with the analytical model, as well as ANN are compared with those extracted from experimental study.

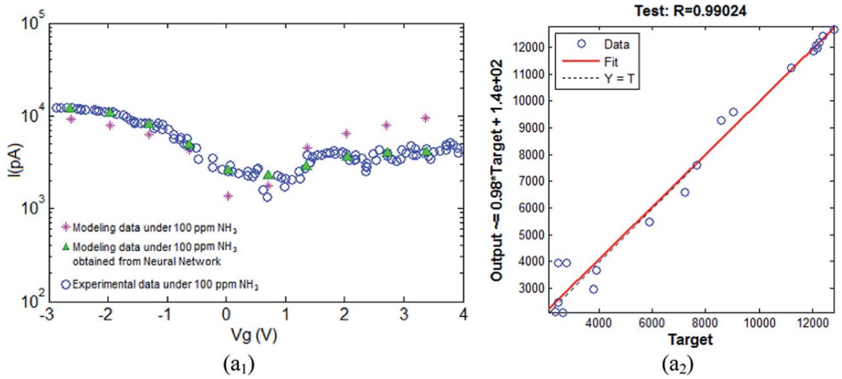

Fig. 9 Comparative study of proposed analytical and ANN models with experimental data at $T = 200$ °C under 100 ppm and the corresponding ANN regression graphs (a$_2$).

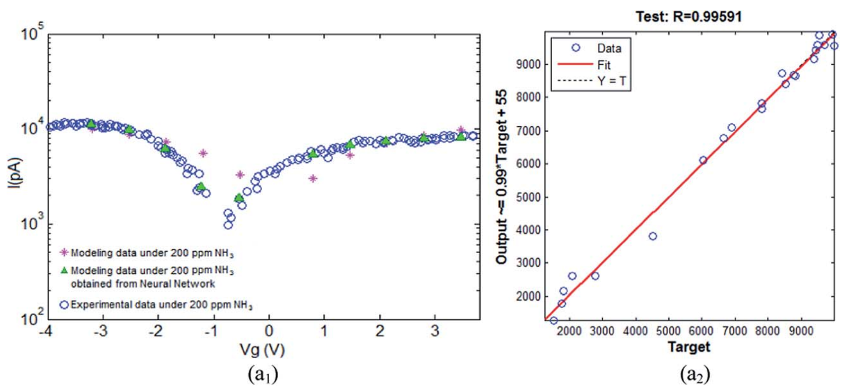

Fig. 10 Comparative study of proposed analytical and ANN models with experimental data at $T = 200$ °C under 200 ppm and the corresponding ANN regression graphs (a$_2$).

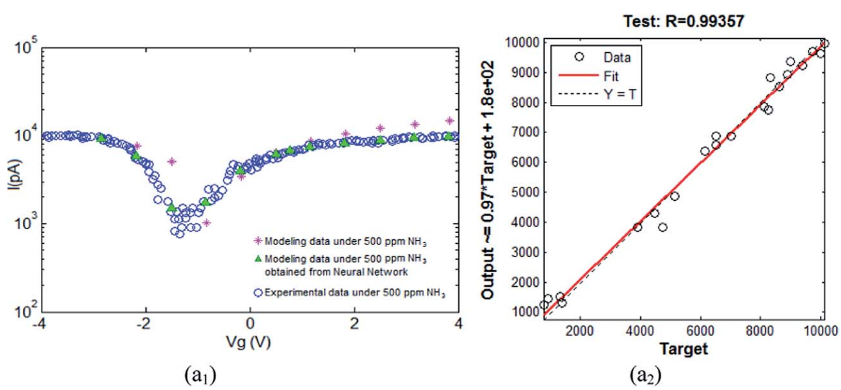

Fig. 11 Comparative study of proposed analytical and ANN models with experimental data at $T = 200$ °C under 500 ppm and the corresponding ANN regression graphs (a$_2$).

As a consequence of the chemical interaction between the NH_3 molecules and the resultant adsorption on the CNT surface which causes electrical charge to be transferred between them and hence changes the carrier concentration, the channel conductivity varies during the process. As observed from Fig. (5a$_1$)–(8a$_1$) corresponding to temperatures of 25, 50, 100, and 150 degrees, respectively, the conductance as a measure of the *I–V* characteristic has increased at higher temperatures. It is also evident from Fig. (5a$_2$)–(8a$_2$) that the proposed ANN model gives to hand better and more accurate estimates of the actual CNT performance in the presence of gas than those provided by the analytical model. This is verified by the fact that the regression values during the calculations of *I–V* points with ANN are remarkably close to 1. Fig. (9)–(11) depict the *I–V* characteristics of CNT at 200 degrees in gas concentrations equal to 100, 200, and 500 ppm, respectively.

Physical and chemical phenomena similar to the previous experiments occur in these cases. The illustrations reveal the fact that when the gas concentration is higher, the CNT conductivity increases. Also in these cases, satisfactory agreement between the ANN results as well as the outstanding value of regression almost equal to 1 prove the ANN model to be superior to the analytical counterpart. This has been shown in Fig. ($9a_2$)–($11a_2$). In Tables 2–5 the data of validation for the analytical model and ANN are presented.

Table 2 Validation parameters for analytical model at different temperature

Gas concentration = 500 ppm				
Temperature (°C)	25	50	100	150
MNS	0.0100	0.0062	0.0068	0.0155
R^2	0.8960	0.9413	0.9247	0.8202
Q^2	0.8190	0.8939	0.8640	0.6278
RSS	0.4351	0.1819	0.0916	0.4060
TSS	4.1831	3.2202	1.2168	2.2577
SSE	0.7012	0.3099	0.1426	0.7122
PRESS	0.7573	0.3418	0.1655	0.8403

Table 3 Validation parameters for analytical model at different gas concentration

Temperature = 200 °C			
Gas concentration (ppm)	100	200	500
MNS	0.0325	0.0392	0.0398
R^2	0.7483	0.7417	0.7321
Q^2	0.3549	0.2429	0.2541
RSS	0.7855	0.8028	2.3183
TSS	3.1207	3.1076	2.3396
SSE	1.8839	2.1930	1.7924
PRESS	2.0131	2.3527	2.5291

Table 4 Model validation parameters for ANN at different temperatures

Gas concentration = 500 ppm				
Temperature (°C)	25	50	100	150
MNS	0.0025	0.0012	0.0011	0.0060
R^2	0.9919	0.9934	0.9969	0.9783
Q^2	0.9783	0.9985	0.9890	0.9441
RSS	0.0773	0.0489	0.0241	0.2566
TSS	9.6007	7.4485	7.6961	11.8104
SSE	0.1961	0.0812	0.0804	0.6391
PRESS	0.2079	0.0854	0.0847	0.6602

Table 5 Model validation parameters for ANN at different gas concentration

Temperature = 200 °C			
Gas concentration (ppm)	100	200	500
MNS	0.0018	0.0017	0.0023
R^2	0.9913	0.9947	0.9889
Q^2	0.9843	0.9918	0.9795
RSS	0.1144	0.0560	0.1500
TSS	13.1572	10.4764	13.4709
SSE	0.2000	0.1817	0.2666
PRESS	0.2072	0.1908	0.2756

4. Conclusion

Two different approaches namely Artificial Neural Network and analytical modelling have been employed in developing models for the *I–V* characteristics of CNTs in exposure to NH_3. It has been demonstrated that the CNT experiences measureable fluctuations in conductance levels when exposed to NH_3. Variations in gas concentration and temperature cause conductance alterations, *i.e.* the higher gas concentration and temperature, the higher conductivity in CNT channel. This interesting phenomenon can be employed in gas detection devices. In the proposed analytical model, two control parameters, namely the temperature control parameters (α) and gas concentration control parameter (β) are incorporated and calculated by iteration method. The ANN model employs the experimental data as the learning data set. Both models are able to produce good results with satisfactory agreement with the extracted experimental data. The ANN model, however, has proved to be able to produce more accurate results than those by the analytical counterpart.

References

1 A. Abdellah, A. Abdelhalim, M. Horn, G. Scarpa and P. Lugli, Scalable Spray Deposition Process for High-Performance Carbon Nanotube Gas Sensors, *IEEE Trans. Nanotechnol.*, 2013, **12**(2), 174–181.

2 A. A. Abolgasim, Master Thesis, Universiti Utara Malaysia, 2008.

3 M. T. Ahmadi, Z. Johari, N. A. Amin, A. H. Fallahpour and R. Ismail, Graphene Nanoribbon Conductance Model in Parabolic Band Structure, *J. Nanomater.*, 2010, **2010**, 12.

4 M. T. Ahmadi, Z. Johari, N. A. Amin, A. H. Fallahpour and R. Ismail, Graphene nanoribbon conductance model in parabolic band structure, *J. Nanomater.*, 2010, **2010**, 12.

5 M. T. Ahmadi, Z. Johari, N. A. Amin, S. M. Mousavi and R. Ismail, Carbon nanotube conductance model in parabolic band structure, IEEE, 2010.

6 M. T. Ahmadi, Z. Johari, N. A. Amin, S. M. Mousavi and R. Ismail. Carbon nanotube conductance model in parabolic band structure, in *Semiconductor Electronics (ICSE), 2010 IEEE International Conference on*. 2010, IEEE.

7 E. Akbari, M. Ahmadi, M. Kiani, H. K. Feizabadi, M. Rahmani and M. Khalid, Monolayer Graphene Based CO_2 Gas Sensor Analytical Model, *J. Comput. Theor. Nanosci.*, 2013, **10**(6), 1301–1304.

8 M. Anantram and F. Leonard, Physics of carbon nanotube electronic devices, *Rep. Prog. Phys.*, 2006, **69**(3), 507.

9 R. H. Baughman, A. A. Zakhidov and W. A. de Heer, Carbon nanotubes–the route toward applications, *Science*, 2002, **297**(5582), 787–792.

10 Q. Cao and J. A. Rogers, Ultrathin Films of Single-Walled Carbon Nanotubes for Electronics and Sensors: A Review of Fundamental and Applied Aspects, *Adv. Mater.*, 2009, **21**(1), 29–53.

11 P. G. Collins, K. Bradley, M. Ishigami and A. Zettl, Extreme oxygen sensitivity of electronic properties of carbon nanotubes, *Science*, 2000, **287**(5459), 1801–1804.

12 S. Datta, *Electronic Transport in Mesoscopic Systems*, Cambridge University Press, Cambridge, UK, 2002.

13 L. Ding, S. Wang, Z. Zhang, Q. Zeng, Z. Wang, T. Pei, L. Yang, X. Liang, J. Shen and Q. Chen, Y-contacted high-performance n-type single-walled carbon nanotube field-effect transistors: scaling and comparison with Sc-contacted devices, *Nano Lett.*, 2009, **9**(12), 4209–4214.

14 R. B. Dingle and R. Dingle, *Asymptotic expansions: their derivation and interpretation*, Academic Press, London, 1973.

15 E. Akbari, M. T. Ahmadi, R. Yusof, M. H. Ghadiry and M. Saeidmanesh, Gas Concentration Effect on Channel Capacitance in Graphene Based Sensors, *J. Comput. Theor. Nanosci.*, 2013, **10**(10), 2449–2452.

16 M. Falvo, G. Clary, R. Taylor, V. Chi, F. Brooks, S. Washburn and R. Superfine, Bending and buckling of carbon nanotubes under large strain, *Nature*, 1997, **389**(6651), 582–584.

17 E. Grossi and M. Buscema, Introduction to artificial neural networks, *Eur. J. Gastroenterol. Hepatol.*, 2007, **19**(12), 1046–1054.

18 P. Gründler, *Chemical sensors: an introduction for scientists and engineers*, Springer, 2007.

19 D. Gunlycke, D. Areshkin and C. White, Semiconducting graphene nanostrips with edge disorder, *Appl. Phys. Lett.*, 2007, **90**, 142104.

20 I. Heller, A. M. Janssens, J. Mannik, E. D. Minot, S. G. Lemay and C. Dekker, Identifying the mechanismof biosensing with carbon nanotube transistors, *Nano Lett.*, 2008, **8**(2), 591–595.

21 S. Iijima, Helical microtubules of graphitic carbon, *Nature*, 1991, **354**(6348), 56–58.

22 A. Javey, J. Guo, Q. Wang, M. Lundstrom and H. Dai, Ballistic carbon nanotube field-effect transistors, *Nature*, 2003, **424**(6949), 654–657.

23 V. Kažukauskas, V. Kalendra, C. Bumby, B. Ludbrook and A. Kaiser, Electrical conductivity of carbon nanotubes and polystyrene composites, *Phys. Status Solidi C*, 2008, **5**(9), 3172–3174.

24 M. J. Kiani, M. Ahmadi, E. Akbari, H. Karimi and F. Che Harun, Graphene Nanoribbon Based Gas Sensor, *Key Eng. Mater.*, 2013, **553**, 7–11.

25 J. Kong, N. R. Franklin, C. Zhou, M. G. Chapline, S. Peng, K. Cho and H. Dai, Nanotube molecular wires as chemical sensors, *Science*, 2000, **287**(5453), 622–625.

26 R. Martel, T. Schmidt, H. R. Shea, T. Hertel and Ph. Avouris, Single-and multi-wall carbon nanotube field-effect transistors, *Appl. Phys. Lett.*, 1998, **73**, 2447.

27 D. W. Patterson, *Artificial neural networks: theory and applications*, Prentice Hall PTR, 1998.

28 N. Peng, Q. Zhang, C. L. Chow, O. K. Tan and N. Marzari, Sensing Mechanisms for Carbon Nanotube Based NH3 Gas Detection, *Nano Lett.*, 2009, **9**(4), 1626–1630.

29 N. M. R. Peres, A. H. Castro Neto and F. Guinea, Conductance quantization in mesoscopic graphene, *Phys. Rev. B: Condens. Matter Mater. Phys.*, 2006, **73**(19), 195411.

30 P. Qi, O. Vermesh, M. Grecu, A. Javey, Q. Wang, H. Dai, S. Peng and K. Cho, Toward large arrays of multiplex functionalized carbon nanotube sensors for highly sensitive and selective molecular detection, *Nano Lett.*, 2003, **3**(3), 347–351.

31 A. Salehi-Khojin, F. Khalili-Araghi, M. A. Kuroda, K. Y. Lin, J.-P. Leburton and R. I. Masel, On the sensing mechanism in carbon nanotube chemiresistors, *ACS Nano*, 2010, **5**(1), 153–158.

32 S. Sivasathya and D. J. Thiruvadigal, *Ab Initio* Study of Carbon Nanotube Transistor-Based Gas Sensor for NO_2 Detection, *Asian J. Chem.*, 2013, **25**, S411–S413.

33 E. Snow, F. Perkins, E. Houser, S. Badescu and T. Reinecke, Chemical detection with a single-walled carbon nanotube capacitor, *Science*, 2005, **307**(5717), 1942–1945.

34 J. R. Stetter, W. R. Penrose and S. Yao, Sensors, chemical sensors, electrochemical sensors, and ECS, *J. Electrochem. Soc.*, 2003, **150**(2), S11–S16.

35 D. Svozil, V. Kvasnicka and J. Pospichal, Introduction to multi-layer feed-forward neural networks, *Chemom. Intell. Lab. Syst.*, 1997, **39**(1), 43–62.

36 K. Uchida, M. Saitoh and S. Kobayashi, Carrier Transport and Stress Engineering in Advanced Nanoscale Transistors From (100) and (110) Transistors To Carbon Nanotube FETs and Beyond, *IEEE Int. Electron Devices Meet., Tech. Dig., 50th*, 2008, 569–572.

37 R. E. Uhrig. Introduction to artificial neural networks, in *Industrial Electronics, Control, and Instrumentation, 1995, Proceedings of the 1995 IEEE IECON 21st International Conference on*, 1995, IEEE.

38 O. Varghese, P. Kichambre, D. Gong, K. Ong, E. Dickey and C. Grimes, Gas sensing characteristics of multi-wall carbon nanotubes, *Sens. Actuators, B*, 2001, **81**(1), 32–41.

39 C. T. White and T. N. Todorov, Carbon nanotubes as long ballistic conductors, *Nature*, 1998, **393**(6682), 240–242.

40 J. L. Xia, F. Chen, J. H. Li and N. J. Tao, Measurement of the quantum capacitance of graphene, *Nat. Nanotechnol.*, 2009, **4**(8), 505–509.

41 K. Xu, X. Tian, C. Wu, J. Liu, M. Li, Y. Sun and F. Wei, Fabrication of single-walled carbon nanotube-based highly sensitive gas sensors, *Sci. China: Technol. Sci.*, 2013, **56**(1), 32–35.

42 H. Yamaura, T. Jinkawa, J. Tamaki, K. Moriya, N. Miura and N. Yamazoe, Indium oxide-based gas sensor for selective detection of CO, *Sens. Actuators, B*, 1996, **36**(1), 325–332.
43 X. Yao, Evolving artificial neural networks, *Proc. IEEE*, 1999, **87**(9), 1423–1447.
44 H. J. Yoon, D. H. Jun, J. H. Yang, Z. Zhou, S. S. Yang and M. M.-C. Cheng, Carbon dioxide gas sensor using a graphene sheet, *Sens. Actuators, B*, 2011, **157**(1), 310–313.
45 Z. Johari, M. T. Ahmadi, D. C. Y. Chek, N. A. Amin and R. Ismail, Modelling of Graphene Nanoribbon Fermi Energy, *J. Nanomater.*, 2010, **2010**, 14.
46 W. Zhang, H. Uchida, T. Katsube, T. Nakatsubo and Y. Nishioka, A novel semiconductor NO gas sensor operating at room temperature, *Sens. Actuators, B*, 1998, **49**(1), 58–62.
47 X.-S. Zhang, Introduction to artificial neural network, in *Neural Networks in Optimization*, Springer, 2000, pp. 83–93.
48 J. M. Zurada, *Introduction to Artificial Neural Systems*, PWS Publishing Company, 1992.